

The Mechanism of Ethylene Dimerization with the $\text{Ti}(\text{OR}')_4/\text{AlR}_3$ Catalytic System: DFT Studies Comparing Metallacycle and Cossee Proposals

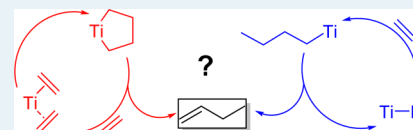
Robert Robinson, Jr., David S. McGuinness,* and Brian F. Yates

School of Chemistry, University of Tasmania, Private Bag 75, Hobart 7001, Australia

Supporting Information

ABSTRACT: The mechanism of ethylene dimerization to 1-butene, as promoted by the $\text{Ti}(\text{OR}')_4/\text{AlR}_3$ catalyst system, has been explored with the aid of density functional theory (DFT) to determine which mechanistic proposal, metallacycle or Cossee–Arlman, is most likely. The theoretical studies predict that the Cossee mechanism has the lowest rate-determining reaction barrier and also that this mechanism is more likely to lead to selective dimerization. In contrast, for the metallacycle mechanism, a higher likelihood of 1-hexene formation is predicted. The possibility of isomerization or codimerization of 1-butene has also been studied according to a Cossee mechanism, with the results obtained in good agreement with previous experiments. As a result of this study and recent experimental results, a Cossee mechanism of dimerization with this catalyst, proceeding via a titanium-hydride intermediate, is considered the most probable route.

KEYWORDS: homogeneous catalysis, ethylene oligomerization, ethylene dimerization, titanium catalysis, theoretical study



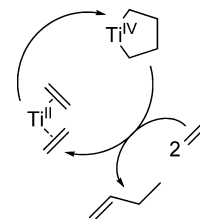
1. INTRODUCTION

The oligomerization of ethylene to short-chain linear α -olefins (LAOs) has been the subject of intense research effort over the past decade.^{1–4} The first three homologues of the series, 1-butene, 1-hexene, and 1-octene, are used on large scale as comonomers for the manufacture of linear low-density polyethylene (LLDPE). Most recent attention has been focused around the discovery of early transition metal catalysts for selective tri- and tetramerization,^{5–9} whereas ethylene dimerization to 1-butene, catalyzed by Ti complexes, has been practiced commercially for many years and can be considered a mature technology.^{1,4,10–13} Nonetheless, the dimerization reaction has received interest of late, with the development of new aryloxy-Ti catalysts^{14,15} and renewed attention to the mechanism of this reaction.^{5,16,17} It is the mechanistic aspects of this reaction that we have considered herein.

The dimerization of ethylene to 1-butene, catalyzed by Ti or Zr alkoxide complexes in combination with triethylaluminum, was discovered by Ziegler and Martin over half a century ago.¹⁸ The system has been improved over the years such that very high activities and selectivity (TOFs approaching $1 \times 10^6 \text{ h}^{-1}$, >93% 1-butene) have been reported.¹¹ The catalyst system $\text{Ti}(\text{OR}')_4/\text{AlR}_3$ ($\text{R}' = \text{C}_1\text{--}\text{C}_8$ alkyl; $\text{R} = \text{C}_1\text{--}\text{C}_6$ *n*-alkyl) appears to be optimal (particularly $\text{Ti}(\text{O}^n\text{Bu})_4/\text{AlEt}_3$),¹¹ although $\text{Ti}(\text{OAr})_4$ ¹⁹ has also been employed. This system was further developed into the commercial Alphabutol process by IFP Energies Nouvelles and Sabic, which now accounts for around 25% of worldwide 1-butene production.^{4,10}

Despite the industrial importance of this catalyst class, the mechanism for 1-butene formation is not well established. The high selectivity of this system is most often attributed to a metallacycle mechanism for ethylene dimerization (Scheme 1)

Scheme 1. Metallacycle Mechanism for Ethylene Dimerization



involving coordination of two ethylene units to a formally Ti(II) species, followed by formation of a Ti(IV) metallacyclopentane.^{4,10,12,20,21} Product release occurs via β -hydride transfer (either stepwise or concerted; see below) to yield 1-butene. Although a metallacycle mechanism is more or less established for ethylene tri- and tetramerization,^{5–9} we have recently questioned the evidence supporting a metallacycle mechanism for dimerization with alkoxy-Ti catalysts.⁵ The main alternative, a conventional Cossee–Arlman mechanism (Scheme 2), has also been suggested in the earlier literature dealing with the $\text{Ti}(\text{OR}')_4/\text{AlR}_3$ system.^{11,22} It is certainly the case that the product distribution arising from this catalyst (1-butene and 1-butene/ethylene codimers) can be rationalized on the basis of a Cossee mechanism with a high rate of chain transfer relative to chain propagation.

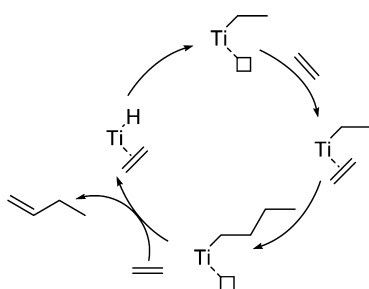
We recently reported experimental studies with $\text{Ti}(\text{O}^n\text{Bu})_4/\text{AlMe}_3$ that support a Cossee mechanism for dimerization while

Received: August 14, 2013

Revised: October 21, 2013

Published: November 8, 2013

Scheme 2. Cossee–Arlman Mechanism for Ethylene Dimerization



strongly disfavoring a metallacycle mechanism.¹⁶ Herein, we have extended this analysis by way of detailed DFT studies of the reaction, considering both possible mechanisms. The relative energetics of both mechanisms are compared, along with their likelihood of leading to selective dimerization.

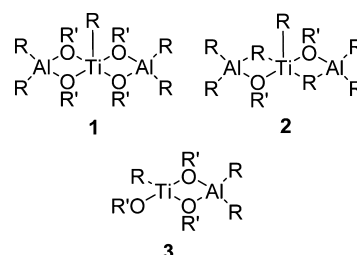
2. THEORETICAL METHODS

All DFT calculations throughout this paper were performed using Gaussian09,²³ utilizing hardware from the National Computational Infrastructure Australian national facility or the Tasmanian Partnership for Advanced Computing facility. Geometry optimizations were performed without symmetry constraints at 298 K and 1 atm using the B3LYP^{24–26} functional in combination with the Stuttgart–Dresden²⁷ (SDD) double- ξ valence basis set and effective core potential (ECP) for Ti and the 6-31G(d) basis set for all other atoms (referred to as BS1). Solvation effects were also incorporated into the geometry optimizations by including the conductor-like polarizable continuum model²⁸ using toluene as the solvent. Analytical frequency calculations were carried out to verify structural optimizations and to obtain Gibbs energy corrections at the same level of theory. All minima (ground-state) structures contained no imaginary frequencies, and all transition structures contained only one imaginary frequency that exhibited vibrational modes consistent with the anticipated reaction pathway (further verified by intrinsic reaction coordinate analysis). Single point energies (SPE) for all structures were calculated with the M06^{29–31} functional with the quadruple- ξ valence def2-QZVP^{32,33} basis set and SDD ECP on Ti, and the 6-311+G(2d,p) basis set on all other atoms (referred to as BS2). The M06 functional was chosen on the basis of benchmarking tests performed by Truhlar and co-workers, in which the averaged error for catalytic energies was evaluated for different functionals.³⁴ This work showed that the M06 functional was associated with relatively low errors for barrier heights relevant to catalysis. The same solvation model as above was incorporated into the SPE calculations. The Gibbs energy (ΔG) values reported throughout this paper were obtained at the M06/BS2//B3LYP/BS1 level with thermal corrections calculated at the B3LYP/BS1 level.

All Ti(III) structures (Cossee mechanism) were optimized in the doublet spin state, and both singlet and triplet spin states were found to be relevant along the metallacycle route (Ti(II) \rightarrow Ti(IV)), as discussed in the text. Minimum energy crossing points (MECPs) between the two surfaces were located using the methodology developed by Harvey and co-workers.³⁵ The barriers for spin state crossing shown in Figure 4 are derived from electronic energies (E_{elec}) at the B3LYP/BS1 level.

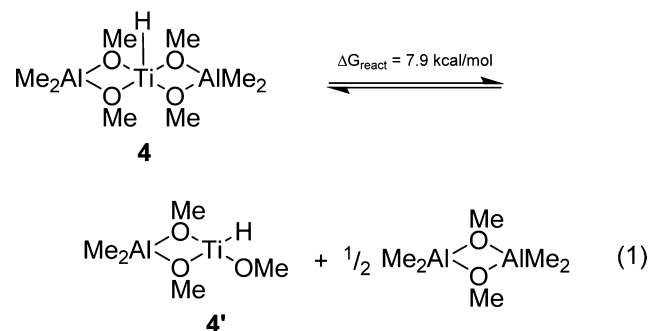
3. RESULTS AND DISCUSSION

In order that a theoretical analysis of the reaction yield reliable results, it is, of course, necessary that a realistic model for the active catalyst be used as input. A number of early experimental studies have been carried out on the system that indicate that a number of structures may be formed, depending upon the Al/Ti ratio.¹¹ At an Al/Ti ratio of 2 (the minimum required to form an active catalyst), ESR analysis indicates the formation of Ti(R)(AlR₂{ μ -OR'}₂)₂ (1), but both Ti(R)(AlR₂{ μ -OR'}{ μ -R})₂ (2) and Ti(R)(OR')({ μ -OR'}₂AlR₂) (3) have also been suggested.^{36–40} Note in each case that the Ti center has been reduced to the formal oxidation state of Ti(III); most experimental studies suggest a Ti(III)-active species at low Al/Ti ratios (<10).¹¹



A number of computational studies of ethylene oligomerization with proposed catalyst 1 (R = Et, R' = Me) in which a Cossee mechanism was considered were, in fact, carried out by Novaro and co-workers in the 1970s.^{22,41,42} We have, therefore, re-examined oligomerization with 1 in more detail, as permitted by modern advances in computational chemistry. Given the similarities between 1 and 2, the latter has been excluded from this study, whereas 3 has been included. A Cossee mode of chain growth and termination is considered first, followed by a metallacycle mechanism.

3.1. Cossee Mechanism. The starting points for the reaction have been taken as the Ti hydrides Ti(H)(AlMe₂{ μ -OMe})₂ (4) and Ti(H)(OMe)(AlMe₂{ μ -OMe})₂ (4'), corresponding to the tri- and bimetallic catalysts, respectively. Complexes 4 and 4' are related to one another by loss/addition of Me₂AlOMe (reaction 1); thus, their relative energies can be



estimated. The Me₂AlOMe moiety would be most stable as a methoxy-bridged dimer,^{39,40} and as such, the ΔG_{react} calculated for reaction 1 reflects this. The bimetallic hydride 4' lies 7.9 kcal·mol⁻¹ above trimetallic 4, and thus, 4 is taken as the zero point on the potential energy surface (PES), shown in Figure 1. In all of the PES plots presented throughout this paper, the solid line corresponds to reaction of the trimetallic system (stationary points X), and the dashed line corresponds to the bimetallic system (stationary points X'). All expected stationary points along the reaction coordinate corresponding to a Cossee

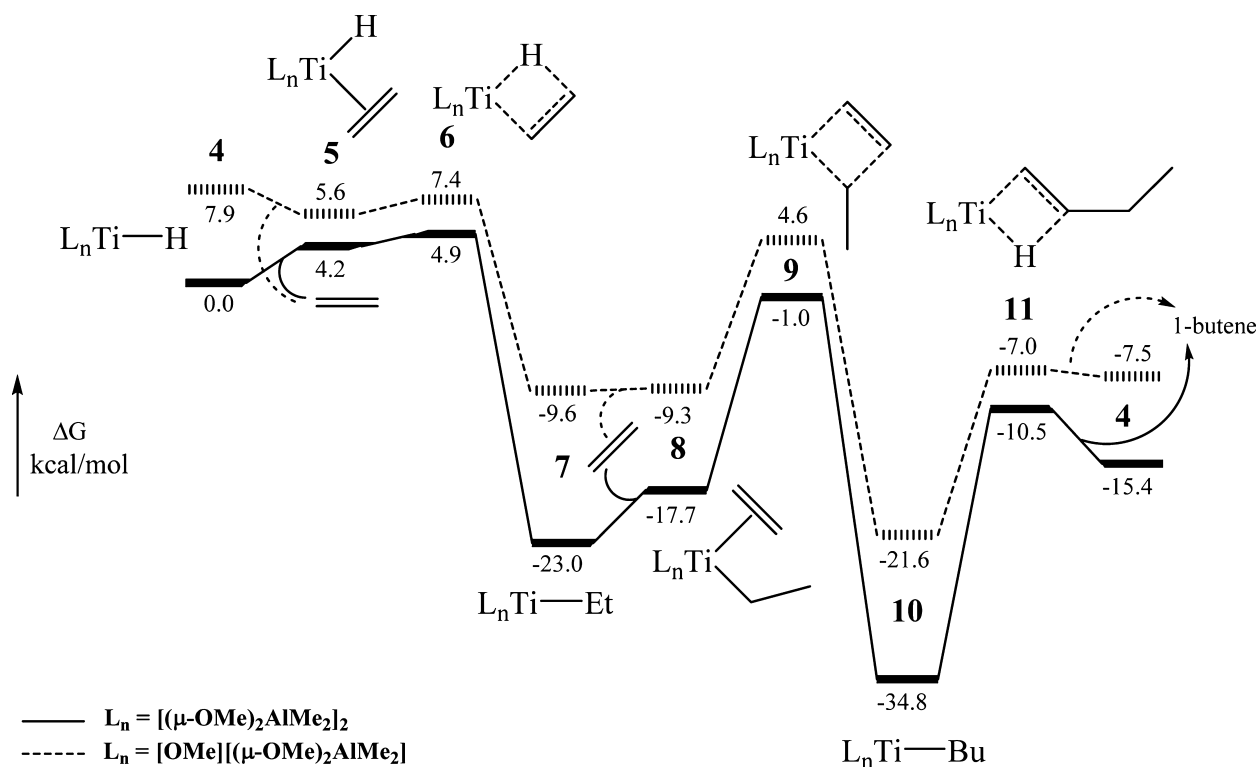


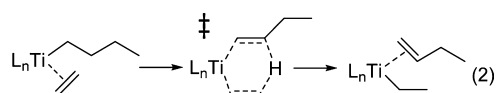
Figure 1. Energy profiles for the dimerization of ethylene ($4/4' + 2$ ethylene $\rightarrow 4/4' + 1$ -butene) via a Cossee mechanism starting from $\text{Ti}(\text{H})(\text{AlMe}_2(\mu\text{-OMe})_2)_2$ (**4**, solid line) and $\text{Ti}(\text{H})(\text{OMe})(\text{AlMe}_2(\mu\text{-OMe})_2)_2$ (**4'**, dashed line). The relative Gibbs energies (ΔG) obtained from M06/BS2//B3LYP/BS1 calculations in toluene are given in $\text{kcal}\cdot\text{mol}^{-1}$.

mechanism were located (Figure 1). It can immediately be seen that the bimetallic mechanism, commencing from **4'** (dashed line), is higher in energy across the whole PES relative to the trimetallic mechanism, commencing from **4** (solid line). As such, the trimetallic mechanism might be considered more probable on the basis of this analysis, although the energy differences are not large and, in particular, are quite similar at the transition structures. It may be that both surfaces could be populated under experimental conditions (and at different Al/Ti ratios).

Figure 1 reveals that the first migratory insertion of ethylene into the Ti-hydrides **4/4'** to yield Ti-ethyl complexes **7/7'** has a very low barrier on both surfaces. The subsequent ethylene insertion to yield Ti-butyl complexes **10** and **10'** and β -hydride elimination to release 1-butene have more substantial barriers. Concentrating on the trimetallic surface (solid line), transition structure (TS) **9** (second insertion) lies $22.0 \text{ kcal}\cdot\text{mol}^{-1}$ above Ti-ethyl **7**, whereas TS **11** (β -H elimination) is $24.3 \text{ kcal}\cdot\text{mol}^{-1}$ above Ti-butyl **10**. As such, the highest activation barrier is predicted to be product release via β -H elimination, although the difference is marginal. In Novaro's early theoretical studies, a trigonal bipyramidal structure for catalyst **1** was considered most likely.⁴² This is confirmed by the present study, in which each stationary point of general structure **1** (**4**, **7**, and **10**; R = H, Et, and Bu, respectively) is best described as such (Figure 2a). An octahedral geometry is adopted at each transition structure as a result of either the interaction of an additional ethylene (insertion TSs **6** and **9**) or the β -hydride transferring to Ti (β -H elimination TS **11**; Figure 2b).

It is also of interest to consider the two possible routes by which chain transfer can occur. Novaro considered that a concerted process involving β -hydride transfer to a coordinated

ethylene monomer was most likely (reaction 2).⁴¹ In Figure 1, the process is shown as occurring via stepwise β -hydride



transfer to Ti, after which a free ethylene could insert (**10** \rightarrow **4**; **4** \rightarrow **7**). The two possibilities are compared in Figure 3. Our calculations suggest that the stepwise process has a considerably lower activation barrier and, as such, is the favored route. This result comes as somewhat of a surprise. The route of direct β -hydride transfer to the monomer was reasonably suggested on the basis of kinetic studies, which show that the rate of β -hydride transfer is dependent upon the ethylene concentration.⁴³ Therefore, at first glance, our predictions seem to conflict with these experimental findings. However, Figure 3 reveals how the rate of β -hydride transfer to ethylene, via the stepwise route, could be dependent upon the concentration of ethylene. The initial β -hydride transfer to generate a Ti-hydride (**10** \rightarrow **4**) is endergonic by $19.4 \text{ kcal}\cdot\text{mol}^{-1}$. As such, this reaction is not spontaneous and in the absence of ethylene will return to the Ti-butyl **10**. Only in the presence of ethylene can the reaction proceed through to Ti-ethyl **7** and 1-butene. As such, we can expect the overall process of chain transfer (**10** \rightarrow **7** + 1-butene) to be dependent on the concentration of ethylene, even when proceeding via a stepwise process. The presence of chain transfer ethylene dependence in oligomerization and polymerization transition metal catalysis is generally accepted to indicate that the concerted hydride-transfer-to-monomer route is operative. It has been shown herein that this is not necessarily the case. This is a notable finding.

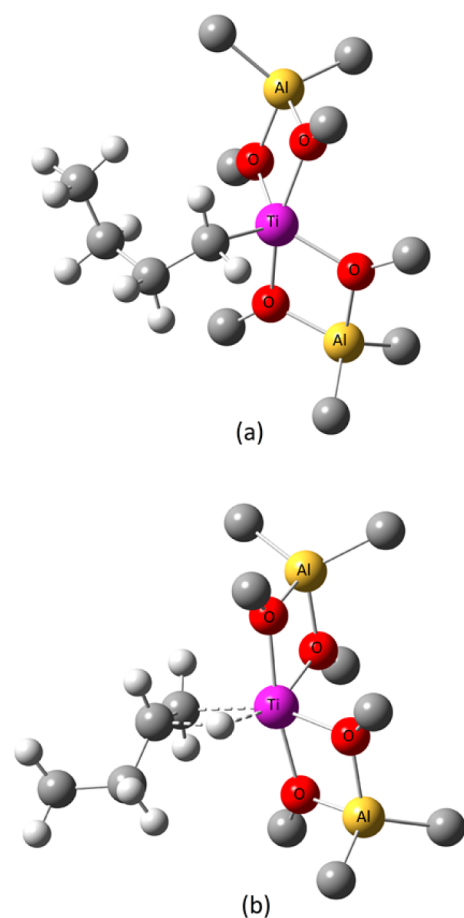
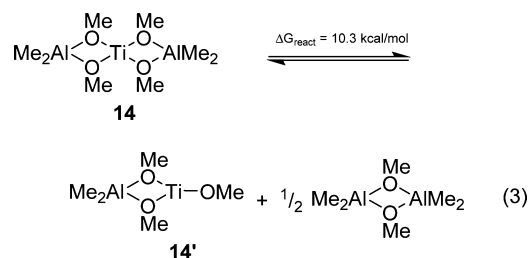


Figure 2. (a) Optimized structure of $\text{Ti}(\mu\text{-Bu})(\text{AlMe}_2\{\mu\text{-OMe}\}_2)_2$ (**10**) and (b) transition structure **11** (β -H elimination). For clarity, only selected hydrogen atoms are shown.

3.2. Metallacycle Mechanism. The formation of metallacycles from group 4 metal(II) precursors and two alkenes is well-known,^{44–47} and the Ti-based ethylene trimerization catalyst of Hesse and co-workers,⁴⁸ which has been extensively studied theoretically,^{49–51} is likewise proposed to operate via a Ti(II)/Ti(IV) cycle. The formation of a Ti(II) complex, such as $\text{Ti}(\text{AlMe}_2\{\mu\text{-OMe}\}_2)_2$ (**14**), has been indicated in experimental studies of the $\text{Ti}(\text{OR}')_4/\text{AlR}_3$ catalyst system at higher Al/Ti ratios.³⁹ Thus, both **14** and $\text{Ti}(\text{OR}')_4/\text{AlR}_3$ (**14'**), which are directly analogous to 4/4', have been studied in this work. Similarly, the relative energies of **14** and **14'** have been calculated on the basis of reaction 3, and again, the bimetallic complex lies higher in energy than the trimetallic complex, this time by $10.3 \text{ kcal}\cdot\text{mol}^{-1}$ (in the triplet spin state; see the discussion below).



The PES for the metallacycle mechanism is shown in Figure 4. The first aspect noted is that the bimetallic and trimetallic surfaces cross at several points along the reaction coordinate and are practically identical in energy at a number of stationary points. This points to the possibility that, should this mechanism be active, the catalyst's ligand set could change at different points throughout the cycle, through loss/addition of Me_2AlOMe . Another possibility is that hemilability might exist in the chelate ligands of the trimetallic catalyst **14**. Reversible dissociation of one O donor in **14** would give a structure very similar to the bimetallic catalyst **14'**, albeit with somewhat

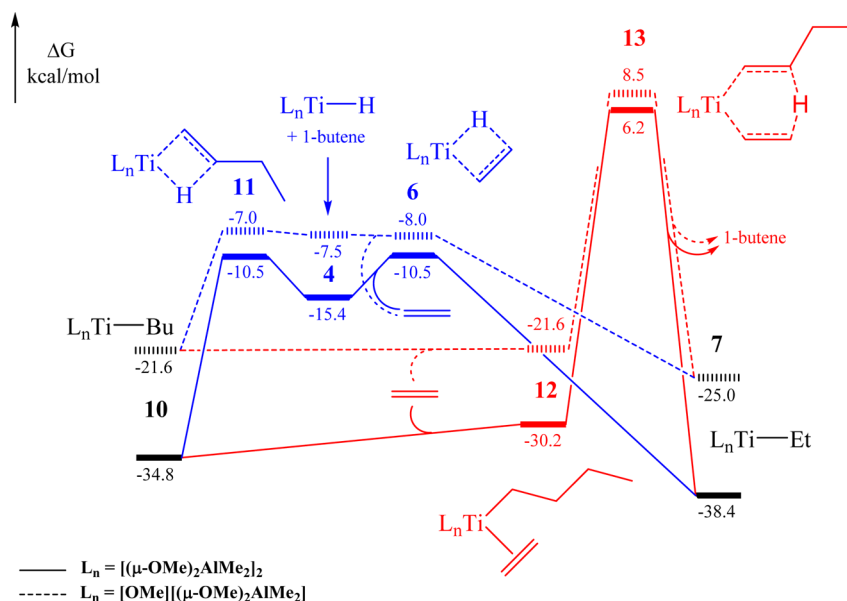


Figure 3. Energy profiles for chain transfer via stepwise (blue line) and concerted (red line) pathways following formation of $L_n\text{TiBu}$ (**10/10'**) from $L_n\text{TiH}$ (**4/4'**) and two ethylene units (as illustrated in Figure 1). The relative Gibbs energies (ΔG) obtained from M06/BS2//B3LYP/BS1 calculations in toluene are given in $\text{kcal}\cdot\text{mol}^{-1}$. All energies relative to $\text{Ti}(\text{H})(\text{AlMe}_2\{\mu\text{-OMe}\}_2)_2$ (**4**) prior to 1-butene formation (left-most **4** in Figure 1) and balanced for ethylene.

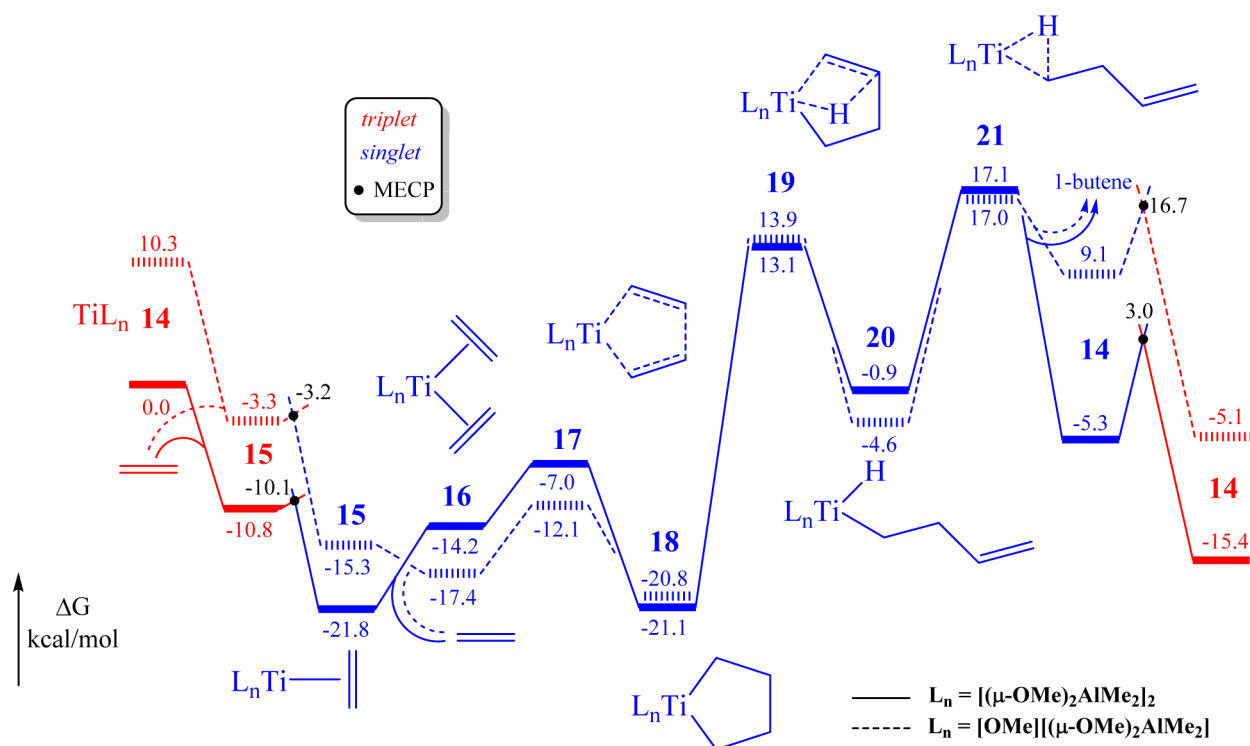


Figure 4. Energy profiles for the dimerization of ethylene ($14/14' + 2$ ethylene $\rightarrow 14/14' + 1$ -butene) via a metallacycle mechanism starting from $\text{Ti}(\text{AlMe}_2\{\mu\text{-OMe}\}_2)_2$ (**14**, solid line) and $\text{Ti}(\text{OMe})(\text{AlMe}_2\{\mu\text{-OMe}\}_2)$ (**14'**, dashed line). The relative Gibbs energies (ΔG) obtained from M06/BS2//B3LYP/BS1 calculations in toluene are given in $\text{kcal}\cdot\text{mol}^{-1}$. MECP barrier heights are derived from B3LYP/BS1 electronic energies.

different electronics. This possibility has not been studied herein; however, it is noted that such ligand hemilability is a feature of Hessen's Ti-based trimerization system, which does operate via a metallacyclic mechanism.⁵²

An analysis of the different spin state possibilities revealed that complexes **14/14'** are most stable as triplets, whereas all other stationary points along the path are lowest in energy in the singlet spin state (a number of stationary points for formally Ti(IV) intermediates could not be located on the triplet surface; see the Supporting Information). As such, there exists the possibility of spin crossover during the reaction, and the MECPs³⁵ located are indicated in Figure 4. The singlet-to-triplet crossover for **14** and **14'** is estimated to have a modest barrier (~ 8 $\text{kcal}\cdot\text{mol}^{-1}$), and as such, this spin flip may not occur in the presence of ethylene if uptake of the monomer is rapid. In other words, if this mechanism were active, spontaneous coordination of ethylene to singlet **14/14'** could lead directly to singlet **15/15'**, which would eliminate all spin crossover in the catalytic cycle. Because we are unsure which possibility is more likely under experimental conditions, the pathway including spin crossover is shown for completeness. Similar spin surface crossing along a metallacycle mechanism for oligomerization (Cr catalyzed) has been documented previously.^{53–55} Although the possibility of spin crossover exists, it does not affect the relevant rate or selectivity-determining barriers, which are discussed below.

Coordination of ethylene to **14** and **14'** is highly exergonic on both surfaces. As illustrated in Figure 5a, coordination of ethylene leads to significant displacement of the hydrogens from that in a planar ethylene geometry. In addition, the C–C bond length has increased from 1.33 Å in free ethylene to 1.45 Å in $\text{Ti}(\text{C}_2\text{H}_4)(\text{AlMe}_2\{\mu\text{-OMe}\}_2)_2$ (**15**) (1.47 Å in $\text{Ti}(\text{C}_2\text{H}_4)(\text{OMe})(\text{AlMe}_2\{\mu\text{-OMe}\}_2)$ (**15'**)). As such, these complexes are

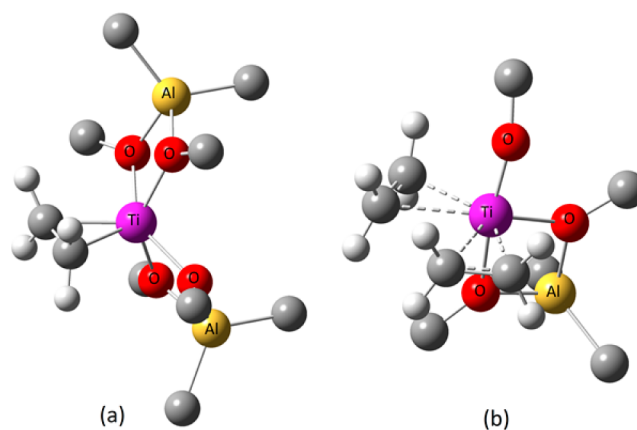


Figure 5. (a) Optimized structures of $\text{Ti}(\text{C}_2\text{H}_4)(\text{AlMe}_2\{\mu\text{-OMe}\}_2)_2$ (**15**) and (b) $\text{Ti}(\text{C}_2\text{H}_4)_2(\text{OMe})(\text{AlMe}_2\{\mu\text{-OMe}\}_2)$ (**16'**). For clarity, only selected hydrogen atoms are shown.

better described as Ti(IV) metallacyclopropanes, rather than Ti(II) ethylene complexes.^{44,56} This is also borne out in the Ti–C bond lengths (2.07–2.09 Å), which are consistent with formal metal–alkyl bonding. Coordination of a second ethylene unit ($\text{Ti}(\text{C}_2\text{H}_4)_2(\text{AlMe}_2\{\mu\text{-OMe}\}_2)_2$ (**16**) and $\text{Ti}(\text{C}_2\text{H}_4)_2(\text{OMe})(\text{AlMe}_2\{\mu\text{-OMe}\}_2)$ (**16'**) leads to binding, which is more olefinic in nature, with both ethylene units equivalent (see, for instance, Figure 5b). It is, therefore, somewhat ambiguous as to how formation of metallacyclopentanes, $\text{Ti}(\text{C}_4\text{H}_8)(\text{AlMe}_2\{\mu\text{-OMe}\}_2)_2$ (**18**) and $\text{Ti}(\text{C}_4\text{H}_8)(\text{OMe})(\text{AlMe}_2\{\mu\text{-OMe}\}_2)$ (**18'**) is best characterized, either as oxidative coupling within a bis-olefin Ti(II) complex to give a Ti(IV) metallacyclopentane or as migratory insertion of ethylene into a Ti(IV) metallacyclopropane complex.⁵⁶ The

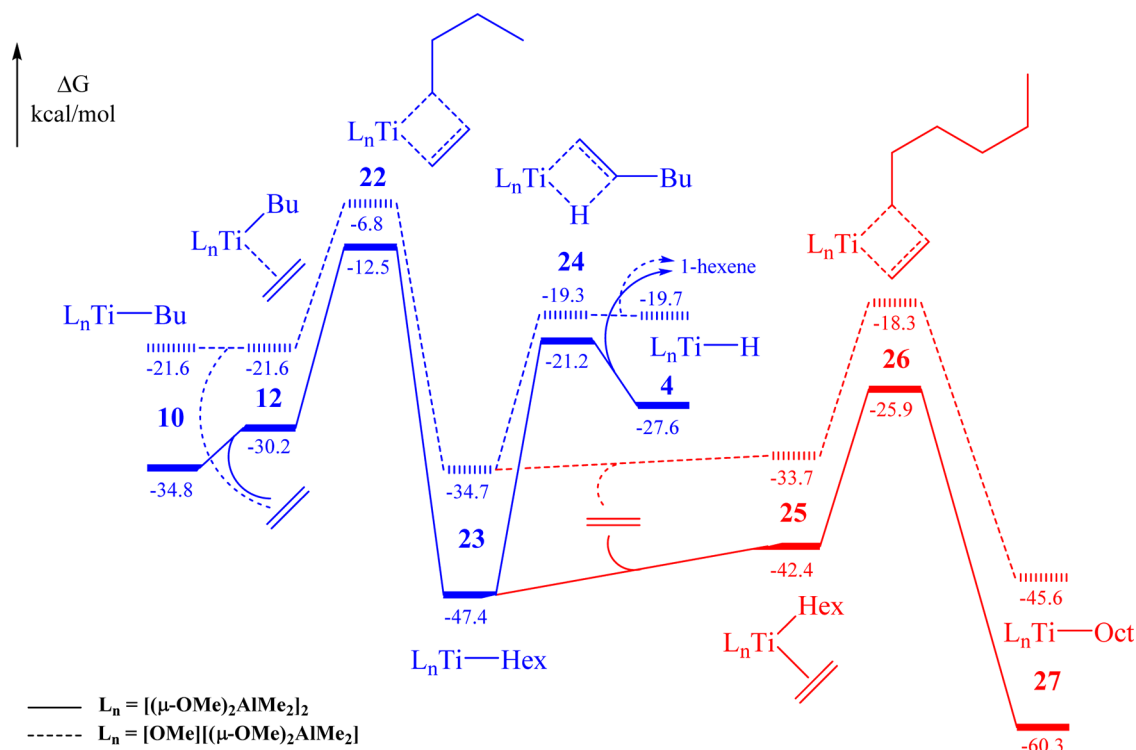


Figure 6. Energy profiles (Cossee mechanism) for chain growth to produce 1-hexene (blue line) and further growth to yield Ti-octyl complexes, $Ti(C_8H_{17})(AlMe_2\{\mu-O)Me\}_2$ (27) and $Ti(C_8H_{17})(OMe)(AlMe_2\{\mu-O)Me\}_2$ (27') (red line). The relative Gibbs energies (ΔG) obtained from M06/BS2//B3LYP/BS1 calculations in toluene are given in kcal·mol⁻¹. All energies relative to $Ti(H)(AlMe_2\{\mu-O)Me\}_2$ (4), as shown in Figure 1.

actual situation probably lies somewhere between the two extremes.

From titanacyclopentanes **18/18'**, β -hydride elimination leads to alkyl-Ti hydrides $Ti(H)(C_4H_7)(AlMe_2\{\mu-O)Me\}_2$ (**20**) and $Ti(H)(C_4H_7)(OMe)(AlMe_2\{\mu-O)Me\}_2$ (**20'**), from which reductive elimination generates 1-butene along with starting structures **14/14'**. The formation of 1-butene was also modeled as proceeding via a concerted β -hydride shift to the opposite α -carbon, which is shown in Figure S2 of the Supporting Information. The concerted route was found to involve a marginally higher barrier, and as such, the discussion will focus on the stepwise route. The reaction barrier from **18** to **14** + 1-butene, at 38 kcal·mol⁻¹, is practically the same on both surfaces. This represents the rate-limiting step of this mechanistic proposal. This barrier along the metallacyclic route is 14 kcal·mol⁻¹ greater than the highest barrier along the Cossee mechanistic route, and as such, the computational results seem to favor the latter proposal. This is in accord with our recent experimental findings.¹⁶

3.3. Product Selectivity. The above results favor a Cossee mechanism on the basis of relative reaction barriers; however, this was not the reason behind our initial skepticism of a metallacycle mechanism, which was rather based upon the likelihood of selectively forming dimers via this route.⁵ It is well established that metallacyclopentanes are considerably more stable than larger metallacycles, which is thought to be due to the constrained geometry of the metallacyclopentane that hinders or even prevents β -hydride elimination.^{57–60} Although intermolecular processes are possible, these, too, appear to be slow.⁶¹ Under these constraints, further ethylene insertion and metallacycle expansion is more likely in most instances. Such a situation is inconsistent with selective dimer formation. It is, therefore, useful to compare the energetics of chain extension

(trimerization and beyond) for both mechanisms to gauge which proposal is more likely to lead to dimer selectivity.

In Figure 6, the PES for further chain growth via the Cossee mechanism is illustrated. We again concentrate on the trimetallic surface, the lower solid line. The decisive barrier is that from Ti-butyl **10** to TS **22** (ethylene insertion), which is 22.3 kcal·mol⁻¹. This is marginally lower than the 24.3 kcal·mol⁻¹ barrier for β -hydride elimination and release of 1-butene (Figure 3). It is therefore tempting to conclude that further ethylene insertion is the favored route. However, although the accuracy of the Minnesota functionals for catalytic reaction barriers is established,³⁴ realistically, the two barriers are too similar to one another to draw firm conclusions. The most that can probably be concluded is that both alternatives are possible; the catalyst model studied could lead to either selective dimerization or higher oligomer/polymer formation, and the switch between the two may be finely balanced. In fact, this conclusion is in some ways consistent with experimental findings. Although the optimized system is highly selective for 1-butene, only minor modifications to conditions or additives are required to destroy this selectivity. Such modifications lead to unselective oligomer formation (Schulz–Flory distributions) or polymer formation.^{11,62,63} It is also worth mentioning that the relative heights of these two barriers are dependent upon the functional employed. With two other functionals evaluated (B3LYP and BP86^{24,64}), the elimination barrier (**10**→**11**) is calculated to be 6–9 kcal·mol⁻¹ lower than that for chain growth (**10**→**22**). As such, these other methods favor dimerization (full details are given in the Supporting Information). Figure 6 reveals that from Ti-hexyl, $Ti(C_6H_{13})(AlMe_2\{\mu-O)Me\}_2$ (**23**), further ethylene insertion has a lower barrier than β -hydride elimination, and the energy differences are a little more decisive in this instance. As such, should Ti-

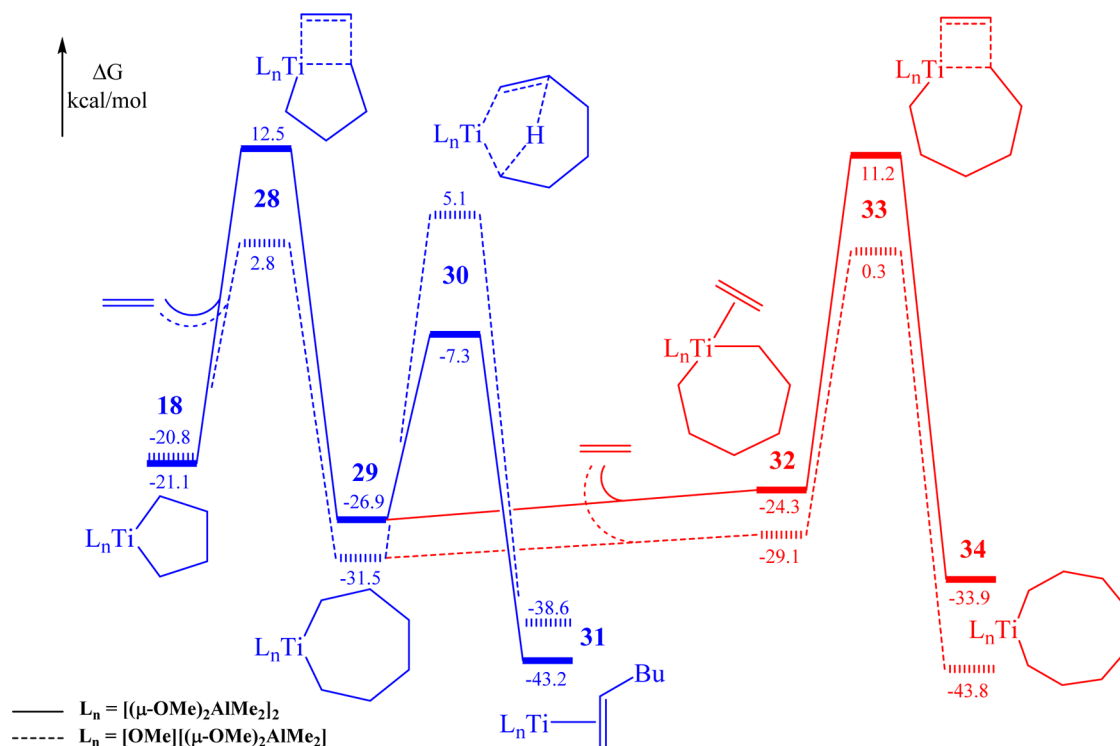


Figure 7. Energy profiles (metallacyclic mechanism) for metallacycle growth to produce 1-hexene (blue line) and further growth to yield titanacyclononane complexes $\text{Ti}(\text{C}_8\text{H}_{16})(\text{AlMe}_2\{\mu\text{-OMe}\}_2)_2$ (**34**) and $\text{Ti}(\text{C}_8\text{H}_{16})(\text{OMe})(\text{AlMe}_2\{\mu\text{-OMe}\}_2)$ (**34'**) (red line). The relative Gibbs energies (ΔG) obtained from M06/BS2//B3LYP/BS1 calculations in toluene are given in kcal·mol⁻¹. All energies relative to $\text{Ti}(\text{AlMe}_2\{\mu\text{-OMe}\}_2)_2$ (**14**), as shown in Figure 4

hexyl **23** form, it might be expected to lead to a distribution of higher oligomers or polymer.

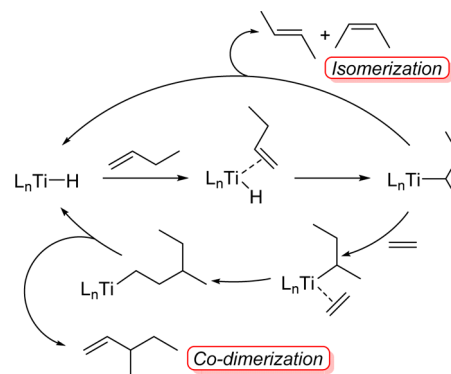
Figure 7 shows the PES for further ethylene insertion into titanacyclopentanes **18** and **18'**. In this case, the lowest barrier for metallacycle expansion (24 kcal·mol⁻¹), via TS **28'** (ethylene insertion), is considerably lower than 1-butene release (Figure 4, ~38 kcal·mol⁻¹). As such, the results are clearer in this case, and it can be concluded that metallacycle expansion is the favored route. This is perhaps not surprising because previous studies have likewise concluded that the high barrier to decomposition of metallacyclopentanes (to 1-butene) is the main reason why further ethylene insertion is preferred.^{49–51} We regard this as the decisive factor that governs selective formation of dimers via metallacycles and renders it unlikely in most cases. However, apparent exceptions do exist in the reported literature.^{65,66} We note that both of these cases involve catalysts with a high degree of coordination saturation. As such, it may be that further coordination and insertion of ethylene is made sufficiently unfavorable that metallacycle decomposition becomes competitive in these instances.

Interestingly, Figure 7 reveals that formation of 1-hexene via TS **30** (β -H transfer) appears to be favored over ring expansion to a metallacyclononane (TSs **33/33'** (ethylene insertion)). The selective formation of 1-hexene via metallacycles is, of course, well-known.^{5,7–9}

3.4. Isomerization and Codimerization of 1-Butene.

One of the major attractions of the Ti-alkoxide-based catalyst system is the very low levels of butene isomerization that occur, such that 2-butene is formed in only minor amounts.¹ According to a Cossee mechanism, isomerization of 1-butene could occur, as shown in Scheme 3, whereby reinsertion of 1-

Scheme 3. Cossee Mechanism for Isomerization and Codimerization



butene in a 2,1-regiochemistry is followed by β -hydride elimination to generate *cis*- and *trans*-2-butene. The possibility of ethylene insertion into the *sec*-butyl-Ti intermediate, which can lead to 3-methyl-1-pentene, is also shown in Scheme 3, effectively representing codimerization of 1-butene with ethylene. The lack of appreciable 2-butene formation has been taken as evidence that Ti-hydride intermediates are not present in the process and that a metallacycle mechanism is more likely.^{4,10} Because we have suggested herein that a mechanism involving hydride intermediates is more probable, a rationalization of the low isomerization activity is now required. The various possibilities for 1-butene reinsertion have been modeled for the trimetallic catalyst and are shown in Figure 8.

The starting point is taken as the Ti-hydride **4** plus free 1-butene. From here, the 1,2-insertion of 1-butene to give *n*-butyl-Ti **10** has a barrier of 4.9 kcal·mol⁻¹. In comparison, the

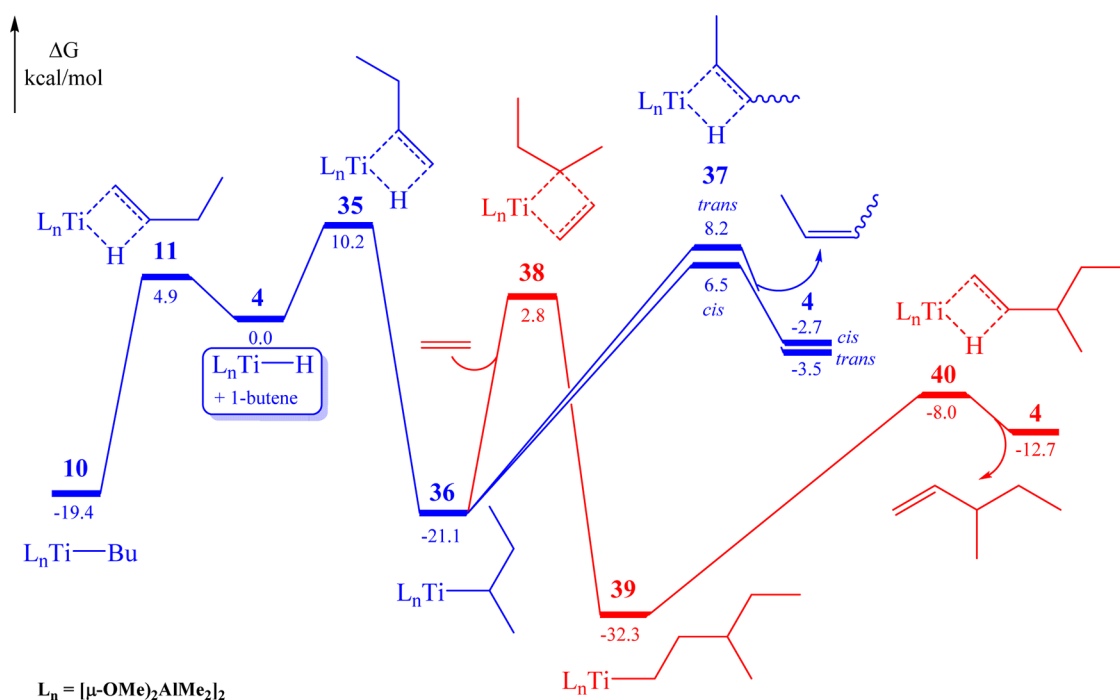


Figure 8. Energy profiles for competing 1-butene isomerization (blue line) and codimerization (red line). The relative Gibbs energies (ΔG) obtained from M06/BS2//B3LYP/BS1 calculations in toluene are given in kcal·mol⁻¹. All energies relative to Ti(H)(AlMe₂{μ-OMe}₂)₂ (4) and free 1-butene.

barrier to 2,1-insertion to give Ti-^{sec}Bu complex, Ti(C₄H₉)-(AlMe₂{μ-OMe}₂)₂ (36) via TS 35 is 10.2 kcal·mol⁻¹. The lower barrier toward 10 suggests that this will be the favored mode of 1-butene reinsertion. In addition, under experimental conditions, the insertion of ethylene would also be favored, so in effect, the 2,1-insertion of 1-butene is competing with two processes with lower barriers. Nonetheless, the formation of 2-methyl-1-pentene, which makes up almost one-third of the C₆ codimers formed experimentally,^{1,10} suggests that 36 does form to some extent. We previously commented¹⁶ that the low level of 2-butenes is somewhat puzzling, given the amount of 3-methyl-1-pentene formed in this reaction. The reason for this now becomes clear in Figure 8. In the presence of a sufficient ethylene concentration, the lowest-barrier route is insertion of ethylene, which leads to 2-methyl-1-pentene. Thus, the formation of the 2-butenes is largely prevented by kinetically preferred ethylene insertion. Although the relative barriers calculated for the competing processes are quite close, the qualitative agreement with experiment is encouraging.

As stated above, the apparent low isomerization ability of this catalyst system has in the past been attributed to a metallacycle mechanism, which lacks a discrete Ti-hydride intermediate. It is therefore worth reconsidering this catalyst attribute in light of the present findings. The results presented above and in Figure 8 suggest that the catalyst does not necessarily lack the ability to promote isomerization. Rather, double bond isomerization is effectively blocked by the presence of ethylene. This occurs at two points: first, the insertion of ethylene into the Ti-hydride is more facile than 2,1-insertion of 1-butene, and second, ethylene insertion into any Ti-^{sec}Bu complex that does form is more facile than β-hydride elimination. This analysis suggests that, in the absence of ethylene, the catalyst might exhibit a propensity for double bond isomerization. This seems to be the case with the commercial catalyst because it has been reported that an

amine is added at the end of the reaction, to prevent isomerization during product separation.²¹

4. SUMMARY AND CONCLUSION

Herein, we have employed experimentally informed model catalysts to theoretically investigate the mechanism of ethylene dimerization with the Ti(OR')₄/AlR₃ catalyst system, a catalyst with considerable industrial importance. The results suggest that both metallacycle and Cossee–Arman mechanisms are capable of oligomerizing ethylene, although the rate-determining barrier for dimerization along the Cossee route is considerably lower than along the metallacycle pathway. The likelihood of forming 1-butene selectively has also been investigated for each pathway, and again, the Cossee route is favored in this regard. Although the theoretical results are not decisive in predicting selective dimerization via this mechanism, they certainly show that catalysts of this nature could exhibit such selectivity. The selective formation of 1-butene via metallacycles is predicted to be less likely, if at all, and the selective formation of 1-hexene seems more probable. Finally, the possibility of 1-butene isomerization and 1-butene/ethylene codimerization has been studied according to a Cossee mechanism. The results show good agreement with experiment, whereby codimerization is observed, but butene isomerization is, for the most part, not. This isomerization reaction appears to be prevented by kinetically preferred ethylene insertion. We believe this study, taken together with our recent experimental results,¹⁶ strongly favors a Cossee mechanism for ethylene dimerization with this catalyst system that proceeds via a discrete, if probably short-lived, Ti-hydride intermediate.

■ ASSOCIATED CONTENT

Supporting Information

Energy profiles for alternative reaction pathways and spin states, and geometries and absolute energies of all stationary

points. This material is available free of charge via the Internet at <http://pubs.acs.org>.

AUTHOR INFORMATION

Corresponding Author

*E-mail: david.mcguinness@utas.edu.au.

Notes

The authors declare no competing financial interest.

ACKNOWLEDGMENTS

We thank the Australian Research Council for financial support through Grant FT100100609 to D.S.M., and the Australian National Computational Infrastructure and Tasmanian Partnership for Advanced Computing for provision of computing resources. We thank Prof. J. N. Harvey for providing the MECP calculation code.

REFERENCES

- (1) Forestière, A.; Olivier-Bourbigou, H.; Saussine, L. *Oil Gas Sci. Technol.* **2009**, *64*, 649.
- (2) Janiak, C.; Blank, F. *Macromol. Symp.* **2006**, *236*, 14.
- (3) Speiser, F.; Braunstein, P.; Saussine, L. *Acc. Chem. Res.* **2005**, *38*, 784.
- (4) Olivier-Bourbigou, H.; Forestière, A.; Saussine, L.; Magna, L.; Favre, F.; Hugues, F. *Oil Gas Eur. Mag.* **2010**, *36*, 97.
- (5) McGuinness, D. S. *Chem. Rev.* **2011**, *111*, 2321.
- (6) van Leeuwen, P. W. N. M.; Clément, N. D.; Tschan, M. J.-L. *Coord. Chem. Rev.* **2011**, *255*, 1499.
- (7) Wass, D. F. *Dalton Trans.* **2007**, 816.
- (8) Agapie, T. *Coord. Chem. Rev.* **2011**, *255*, 861.
- (9) Dixon, J. T.; Green, M. J.; Hess, F. M.; Morgan, D. H. *J. Organomet. Chem.* **2004**, *689*, 3641.
- (10) Commereuc, D.; Chauvin, Y.; Gaillard, J.; Léonard, J.; Andrews, J. *Hydrocarb. Process* **1984**, *63*, 118.
- (11) Al-Sa'doun, A. W. *App. Catal., A* **1993**, *105*, 1.
- (12) Al-Jarallah, A. M.; Anabtawi, J. A.; Siddiqui, M. A. B.; Aitani, A. M.; Al-Sa'doun, A. W. *Catal. Today* **1992**, *14*, 1.
- (13) Muthukumar Pillai, S.; Ravindranathan, M.; Sivaram, S. *Chem. Rev.* **1986**, *86*, 353.
- (14) Cazaux, J.-B.; Braunstein, P.; Magna, L.; Saussine, L.; Olivier-Bourbigou, H. *Eur. J. Inorg. Chem.* **2009**, 2942.
- (15) Grasset, F.; Cazaux, J.-B.; Magna, L.; Braunstein, P.; Olivier-Bourbigou, H. *Dalton Trans.* **2012**, *41*, 10396.
- (16) Suttill, J. A.; McGuinness, D. S. *Organometallics* **2012**, *31*, 7004.
- (17) Suttill, J. A.; McGuinness, D. S.; Pichler, M.; Gardiner, M. G.; Morgan, D. H.; Evans, S. J. *Dalton Trans.* **2012**, *41*, 6625.
- (18) Ziegler, K.; Martin, H. U.S. Patent 2943125 1960.
- (19) Yamada, S.; Ono, I. *Bull. Jpn. Pet. Inst.* **1970**, *12*, 160.
- (20) Bre, A.; Chauvin, Y.; Commereuc, D. *Nouv. J. Chim.* **1986**, *10*, 535.
- (21) Chauvin, Y.; Olivier, H. In *Applied Homogenous Catalysis with Organometallic Compounds*; Cornils, B., Herrmann, W. A., Eds.; VCH: Weinheim, 1996; Vol. 1, p 258.
- (22) Novaro, O.; Chow, S.; Magnouat, P. *J. Catal.* **1976**, *41*, 91.
- (23) Frisch, M. J.; Trucks, G. W.; Schlegel, H. B.; Scuseria, G. E.; Robb, M. A.; Cheeseman, J. R.; Scalmani, G.; Barone, V.; Mennucci, B.; Petersson, G. A.; Nakatsuji, H.; Caricato, M.; Li, X.; Hratchian, H. P.; Izmaylov, A. F.; Bloino, J.; Zheng, G.; Sonnenberg, J. L.; Hada, M.; Ehara, M.; Toyota, K.; Fukuda, R.; Hasegawa, J.; Ishida, M.; Nakajima, T.; Honda, Y.; Kitao, O.; Nakai, H.; Vreven, T.; Montgomery, J. A., Jr.; Peralta, J. E.; Ogliaro, F.; Bearpark, M.; Heyd, J. J.; Brothers, E.; Kudin, K. N.; Staroverov, V. N.; Kobayashi, R.; Normand, J.; Raghavachari, K.; Rendell, A.; Burant, J. C.; Iyengar, S. S.; Tomasi, J.; Cossi, M.; Rega, N.; Millam, J. M.; Klene, M.; Knox, J. E.; Cross, J. B.; Bakken, V.; Adamo, C.; Jaramillo, J.; Gomperts, R.; Stratmann, R. E.; Yazyev, O.; Austin, A. J.; Cammi, R.; Pomelli, C.; Ochterski, J. W.; Martin, R. L.; Morokuma, K.; Zakrzewski, V. G.; Voth, G. A.; Salvador, P.;

- Dannenberg, J. J.; Dapprich, S.; Daniels, A. D.; Farkas, Ö.; Foresman, J. B.; Ortiz, J. V.; Cioslowski, J.; Fox, D. J. *Gaussian 09, revision A.1*; Gaussian, Inc.: Wallingford, CT, 2009.
- (24) Becke, A. D. *Phys. Rev. A* **1988**, *38*, 3098.
- (25) Becke, A. D. *J. Chem. Phys.* **1993**, *98*, 5648.
- (26) Lee, C.; Yang, W.; Parr, R. G. *Phys. Rev. B* **1988**, *37*, 785.
- (27) Andrae, D.; Häussermann, U.; Dolg, M.; Stoll, H.; Preuss, H. *Theor. Chim. Acta* **1990**, *77*, 123.
- (28) Barone, V.; Cossi, M. *J. Phys. Chem. A* **1998**, *102*, 1995.
- (29) Zhao, Y.; Schultz, N. E.; Truhlar, D. G. *J. Chem. Theory Comput.* **2006**, *2*, 364.
- (30) Zhao, Y.; Truhlar, D. G. *J. Chem. Phys.* **2006**, *125*, 194101.
- (31) Zhao, Y.; Truhlar, D. G. *J. Phys. Chem. A* **2006**, *110*, 13126.
- (32) Weigend, F.; Ahlrichs, R. *Phys. Chem. Chem. Phys.* **2005**, *7*, 3297.
- (33) Weigend, F.; Furche, F.; Ahlrichs, R. *J. Chem. Phys.* **2003**, *119*, 12753.
- (34) Yang, K.; Zheng, J.; Zhao, Y.; Truhlar, D. G. *J. Chem. Phys.* **2010**, *132*, 164117.
- (35) Harvey, J. N.; Aschi, M.; Schwarz, H.; Koch, W. *Theor. Chem. Acc.* **1998**, *99*, 95.
- (36) Dzhabiev, T. S.; Sabrova, R. D.; Shilov, A. E. *Kinet. Katal.* **1964**, *5*, 441.
- (37) Angelescu, E.; Nicolau, C.; Simon, Z. *J. Am. Chem. Soc.* **1966**, *88*, 3910.
- (38) Hirai, H.; Hiraki, K.; Noguchi, I.; Makishima, S. *J. Polym. Sci., Part A* **1970**, *8*, 147.
- (39) Christenson, C. P.; May, J. A.; Freyer, L. E. In *Transition Metal Catalyzed Polymerizations: Alkenes and Dienes*; Quirk, R. P., Ed.; Harwood Academic: New York, 1983, p 763.
- (40) Uetsuki, M.; Fujiwara, Y. *Bull. Chem. Soc. Jpn.* **1976**, *49*, 3530.
- (41) Novaro, O.; Chow, S.; Magnouat, P. *Polym. Lett.* **1975**, *13*, 761.
- (42) Novaro, O.; Chow, S.; Magnouat, P. *J. Catal.* **1976**, *42*, 131.
- (43) Henrici-Olivé, G.; Olivé, S. *J. Polym. Sci., Polym. Lett. Ed.* **1974**, *12*, 39.
- (44) Cohen, S. A.; Auburn, P. R.; Bercaw, J. E. *J. Am. Chem. Soc.* **1983**, *105*, 1136.
- (45) Alt, H. G.; Denner, C. E.; Thewalt, U.; Rausch, M. D. *J. Organomet. Chem.* **1988**, *356*, C83.
- (46) Spencer, M. D.; Wilson, S. R.; Girolami, G. S. *Organometallics* **1997**, *16*, 3055.
- (47) Buchwald, S. L.; Nielsen, R. B. *Chem. Rev.* **1988**, *88*, 1047.
- (48) Deckers, P. J. W.; Hessen, B.; Teuben, J. H. *Organometallics* **2002**, *21*, 5122.
- (49) Tobisch, S.; Ziegler, T. *Organometallics* **2003**, *22*, 5392.
- (50) de Bruin, T. J. M.; Magna, L.; Raybaud, P.; Toulhoat, H. *Organometallics* **2003**, *22*, 3404.
- (51) Blok, A. N. J.; Budzelaar, P. H. M.; Gal, A. W. *Organometallics* **2003**, *22*, 2564.
- (52) Otten, E.; Batinas, A. A.; Meetsma, A.; Hessen, B. *J. Am. Chem. Soc.* **2009**, *131*, 5298.
- (53) Yang, Y.; Liu, Z.; Zhong, L.; Qiu, P.; Dong, Q.; Cheng, R.; Vanderbilt, J.; Liu, B. *Organometallics* **2011**, *30*, 5297.
- (54) Liu, Z.; Cheng, R.; He, X.; Wu, X.; Liu, B. *J. Phys. Chem.* **2012**, *116*, 7538.
- (55) Liu, Z.; Cheng, R.; He, X.; Liu, B. *ACS Catal.* **2013**, *3*, 1172.
- (56) Steigerwald, M. L.; Goddard, W. A., III. *J. Am. Chem. Soc.* **1985**, *107*, 5027.
- (57) McDermott, J. X.; White, J. F.; Whitesides, G. M. *J. Am. Chem. Soc.* **1973**, *95*, 4451.
- (58) McDermott, J. X.; White, J. F.; Whitesides, G. M. *J. Am. Chem. Soc.* **1976**, *98*, 6521.
- (59) McDermott, J. X.; Whitesides, G. M. *J. Am. Chem. Soc.* **1974**, *96*, 947.
- (60) McDermott, J. X.; Wilson, M. E.; Whitesides, G. M. *J. Am. Chem. Soc.* **1976**, *98*, 6529.
- (61) Miller, T. M.; Whitesides, G. M. *Organometallics* **1986**, *5*, 1473.
- (62) Henrici-Olivé, G.; Olivé, S. *Angew. Chem., Int. Ed.* **1970**, *9*, 243.
- (63) Henrici-Olivé, G.; Olivé, S. *Angew. Chem., Int. Ed.* **1971**, *10*, 105.
- (64) Perdew, J. P. *Phys. Rev. B.* **1986**, *33*, 8822.

- (65) McLain, S. J.; Schrock, R. R. *J. Am. Chem. Soc.* **1978**, *100*, 1315.
(66) You, Y.; Girolami, G. S. *Organometallics* **2008**, *27*, 3172.